Journal of Organometallic Chemistry, 335 (1987) 395–411
Elsevier Sequoia S.A., Lausanne – Printed in The Netherlands

Molecular orbital study of stereoselective addition of ligands to the hydride, alkyl, and halide complexes of iridium and zirconium. The question of central versus lateral attack

Longgen Zhu and Nenad M. Kostić*

Department of Chemistry, Iowa State University, Ames, Iowa 50011 (U.S.A.)

(Received November 5th, 1986; in revised form April 25th, 1987)

Abstract

Electronic structures of $Ir(N(SiH_3)_2)(PH_3)_2H_2$, Cp_2ZrMe_2, Cp_2ZrH_2, and Cp_2ZrCl_2 complexes and stereoselectivity of CO addition to each of them are studied by the nonparametrized Fenske–Hall method. A new measure of the interaction between reactants, designated ΔE, is defined and used to calculate energy profiles of the carbonylation reactions. Stereoselectivity seems to be controlled by the composition and localization of the frontier orbitals. The experimental observations are explained successfully: the first two complexes undergo lateral attack, the third one undergoes central attack, and the fourth one is unreactive. The unreactivity of the chloro complex is attributed to the repulsion between the lone pairs of the Cl and CO ligands. The nature of the frontier orbitals, and consequently the preferred approach of an incoming ligand, depends markedly on the LZrL angle: the LUMO is localized laterally when the angle is acute and centrally when it is obtuse. Experiments are proposed that may test the correlation between the facility of ligand-addition reactions and the localization of the frontier orbitals.

I. Introduction

Transition-metal hydride complexes are involved in various catalytic processes as reactive intermediates [1]. Research into synthesis and reactivity of these complexes represents a flourishing branch of contemporary organometallic and inorganic chemistry [2]. Studies of hydrogen activation [3] were stimulated by the recent discovery of transition-metal complexes containing η^2-H_2 ligands [4–15]. Since hydrogen atoms bonded to early transition metals have hydridic character and act as nucleophiles toward unsaturated ligands such as CO [16,17] and olefins [18], complexes of early transition metals hold promise as potential homogeneous catalysts for the conversion of synthetic gas into various products.

0022-328X/87/$03.50

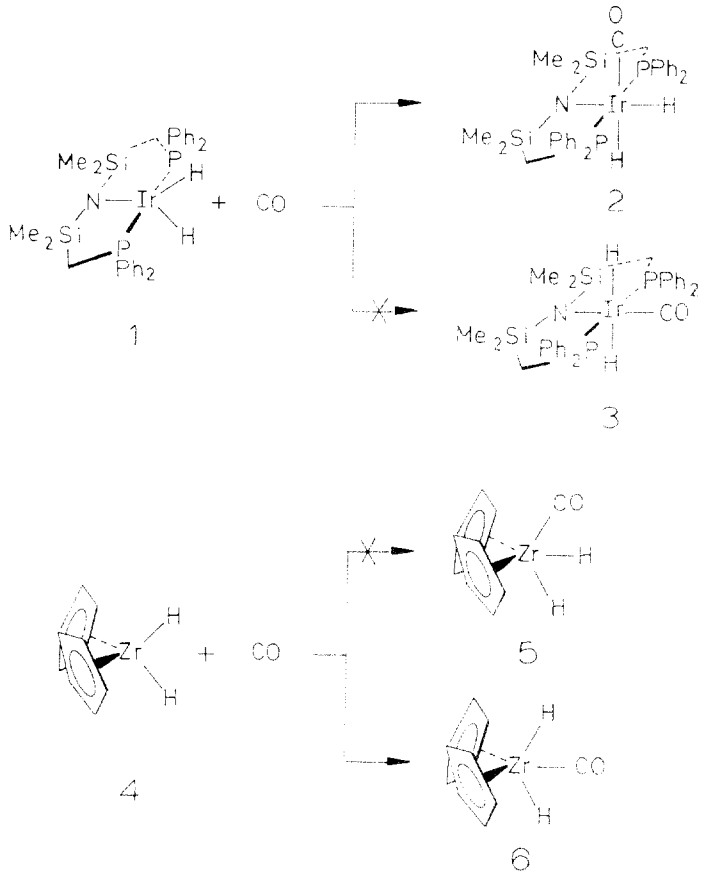

Scheme 1

Two intriguing carbonylation reactions are shown in Scheme 1. They are stereoselective and, moreover, opposite from each other: the CO ligand adds laterally to the $[Ir]H_2$ complex [19], but centrally to the $[Zr]H_2$ complex [16,20]. (The brackets contain the metal and ligands that are not involved in the reaction. The Zr complex actually contains permethylated ligands Cp^* [16,20], but Cp rings are drawn for clarity.) Various other two-electron donors behave analogously: PMe_3 [19] and other ligands [21] add laterally to the $[Ir]H_2$ complex; PF_3 [20], $Cp_2W(CO)$ [22], and RNC [23] add centrally to the $[Zr]H_2$ complex. Although additions of all of these ligands may not be kinetically controlled, the reactions shown in Scheme 1 seem to be rather general. This study is concerned mainly with hydride complexes, but interesting differences in reactivity and stereoselectivity of homologous alkyl and halide complexes are examined as well.

The electronic structures of the metal complexes are elucidated by the nonparametrized Fenske–Hall method for molecular orbital calculations. The stereoselectivity of carbonylation reactions is attributed to the frontier orbitals in the $[M]L_2$ complexes; the orbital composition and localization, in turn, depend on the geometric structure of the complexes. The question of central versus lateral attack of

nucleophiles to complexes Cp_2ZrL_2, wherein L are ligands other than H, has recently been treated in several mechanistic [24–27] and quantum-chemical [28,29] studies. The complexes wherein L is H have been studied less in this regard [30,31].

II. Bonding in the iridium complexes

In order to facilitate the analysis of bonding and of chemical reactions, each complex molecule is constructed from the chemically meaningful fragments, which, in turn, are built from subfragments and ultimately from atoms. Since the tridentate amidodiphosphine ligand is unaffected by the reactions, the $Ir(N(SiH_3)_2)(PH_3)_2$ fragment is kept invariant and the structural changes confined to the unidentate ligands, H and CO. The same appraoch is taken in the study of zirconium complexes, to be discussed below.

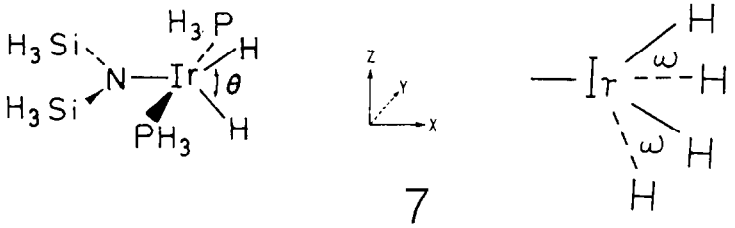

7

IIA. The [Ir]H_2 complex. In the optimal structure of this compound the IrH_2 and PNP planes are perpendicular to each other; the optimal HIrH angle θ in C_{2v} symmetry is 90°. The two H ligands are 2.33 Å apart and virtually not bonded to each other. As Fig. 1 shows, two principal interactions between the [Ir] and H_2 fragments are σ donation of A_1 symmetry, $\sigma a_1 \rightarrow 2a_1$, and π back-donation of B_2 symmetry, $\sigma^* b_2 \leftarrow 1b_2$ and $\sigma^* b_2 \leftarrow 2b_2$. The composition of the most important molecular orbitals is presented in Table 1. The partial antibonding character of the HOMO, A_1^{non}, stems from two factors: the slight four-electron, repulsive interaction between the fragment orbitals $1a_1$ and σa_1; and admixture into the HOMO of a lower-lying orbital of a_1 symmetry in the metal fragment, which is not included in Fig. 1.

The contributions to the Ir–H bonding from the σ and π interactions can be inferred from Tables 1 and 2. The π bonding, of B_2 symmetry, provides a greater mixing of the fragment orbitals, a lower energy of the bonding molecular orbital, and greater overlap populations. The difference between the dihydride complex $[Ir]H_2$ and the dihydrogen complex $W(CO)_3(P\text{-}i\text{-}Pr_3)_2(\eta^2\text{-}H_2)$, in which the η^2-H_2 ligand acts essentially as a pure σ donor [32], can be explained by the arguments of Saillard and Hoffmann [33].

IIB. The frontier orbitals and distortion of the [Ir]H_2 complex. Both of the frontier orbitals lie in the HIrH (or xz) plane, as depicted in **8** and **9**. The HOMO is antibonding with respect to the Ir–N interaction, whereas the LUMO is antibonding with respect to the Ir–H interactions. We examined two motions of the H ligands in the xz plane: change in the bond angle, θ, in which the local C_{2v} symmetry is preserved; and pivoting by angle ω, in which the symmetry is reduced to C_1. The angles are defined in **7**. These distortions do not alter qualitatively the spatial characteristics of the frontier orbitals, shown in **8** and **9**. The HOMO lies

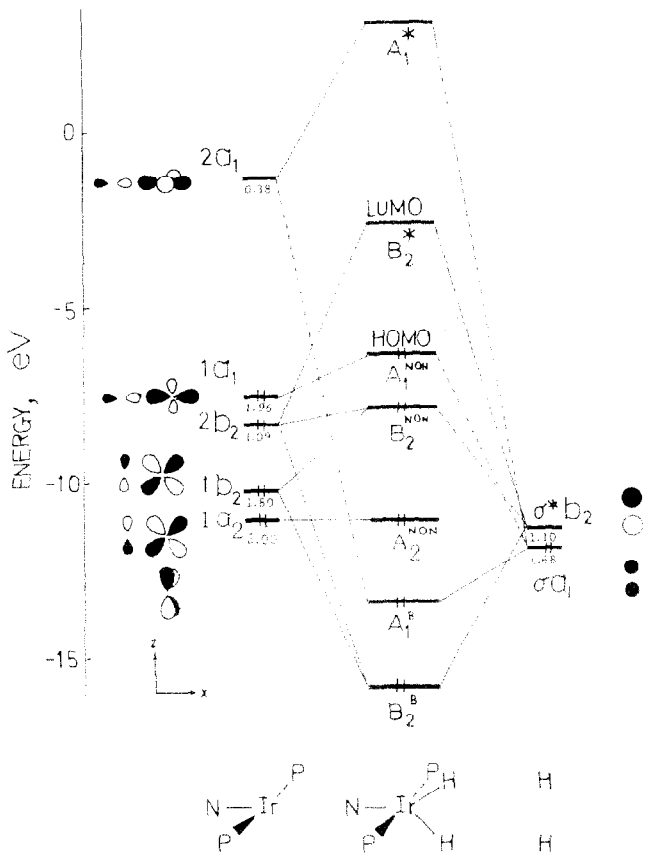

Fig. 1. Molecular-orbital diagram for $[Ir(N(SiH_3)_2(PH_3)_2]H_2$ wherein the HIrH angle is 90°. The numbers indicate populations of the fragment orbitals in electron units; the dashed lines represent minor contributions of the fragment orbitals to the molecular orbitals.

along the x and z axes, with a large lobe protruding between the H ligands, in the central (x) direction; the LUMO lies between the x and z axes, with its lobes protruding beside the H ligands, in the lateral directions. A small but significant

HOMO 8 LUMO 9

preference exists for a distortion toward square-pyramidal structure, as expected for a pentacoordinate, low-spin d^6 complex [34,35]. Since pivoting removes any symmetry, an attempt to follow the evolution of molecular orbitals and to attribute

Table 1

Energies and compositions of the important molecular orbitals in $Ir(N(SiH_3)_2)(PH_3)_2H_2$ wherein the HIrH bond angle is 90°

MO	ϵ (eV)	Ir	H	Other
$A_1^{\star}$	0.19	54% d_{xz}	28% 1s	
$B_2^{\star}$, LUMO	−2.57	50% d_{xz}	44% 1s	
A_1^{non}, HOMO	−6.39	36% d_{z^2}	4% 1s	N, 48% p_σ
B_2^{non}	−7.93		4% 1s	N, 89% p_π
A_1^{b}	−13.48	5% $d_{x^2-y^2}$	44% 1s	P, 19% p_σ
B_2^{b}	−15.89	36% d_{xz}	38% 1s	Si, 10% p_π

Table 2

Overlaps and overlap populations involving four orbitals of the Ir-containing fragment and two orbitals of the dihydride fragment in $Ir(N(SiH_3)_2)(PH_3)_2H_2$ wherein the HIrH bond angle is 90°

	Overlap		Overlap population, in e	
	σa_1	$\sigma^{\star} b_2$	σa_1	$\sigma^{\star} b_2$
$2a_1$	0.241		0.267	
$1a_1$	0.124		−0.017	
$2b_2$		−0.213		0.318
$1b_2$		−0.167		0.085

structural preference to particular interaction is unwarranted. The optimal structure corresponds to $\omega = 20°$. As Fig. 2 shows, the re-orientation of the HOMO and LUMO upon pivoting of the H ligand is relatively small. The activation energy for

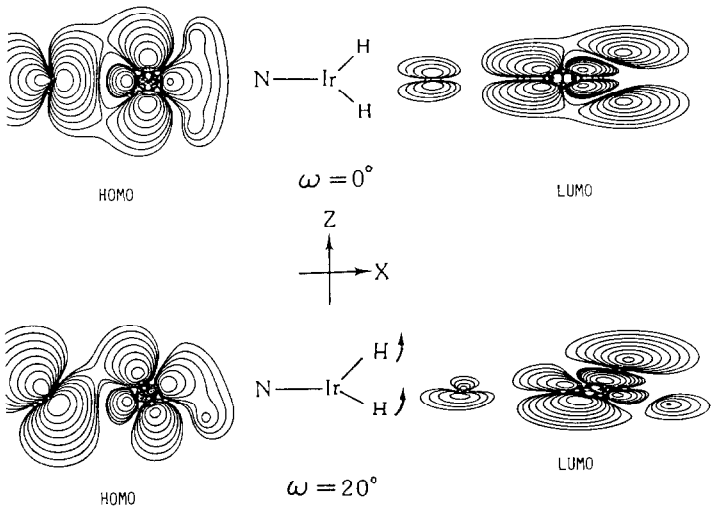

Fig. 2. Contour plots of the HOMO and LUMO in $Ir(N(SiH_3)_2)(PH_3)_2H_2$. The pivot angle, ω, defined in 7, is 0 and 20°; the HIrH bond angle, θ, is 90°.

the interconversion of the two equivalent C_1 isomers, as shown in **10**, is approximately 6 kcal mol^{-1}.

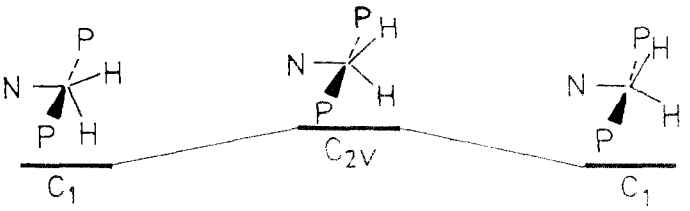

10

Although the ^1H NMR spectrum of the $[Ir]H_2$ complex is compatible with the rigid C_{2v} structure [19], a possibility of facile interchange between the two C_1 structures is worth considering. Complexes $[Ir(N(SiMe_2CH_2PR_2)_2)]MeI$ and $[Ir(N(SiMe_2CH_2PPh_2)_2)]Me(CH_2CMe_3)$, homologs of $[Ir]H_2$, are distorted toward square-pyramidal configuration in the solid state [36–38]. Since $[Ir]Me(CH_2CMe_3)$ and $[Ir]Me_2$ in solution proved indistinguishable by the nuclear Overhauser effect [38], the structure of the latter molecule, too, probably is distorted by pivoting [39*]. These experimental studies seem to corroborate the notion that the $[Ir]H_2$ complex adopts the structure with C_1 local symmetry.

III. Carbonylation of $[Ir]H_2$

We examined thoroughly the reaction with CO and, by less comprehensive series of calculations, confirmed the reaction with PH_3 to be similar to carbonylation in all important respects. The stereoselectivity seems to be governed by the localization of the frontier orbitals in $[Ir]H_2$, shown in **8** and **9**. The central attack of CO is unfavorable on two counts. First, as shown in **11**, it leads to a repulsive, four-electron interaction between the filled HOMO's of the two reactants. Second, the LUMO has no $d_{x^2-y^2}$ character, and no lobe in the x direction, for any plausible

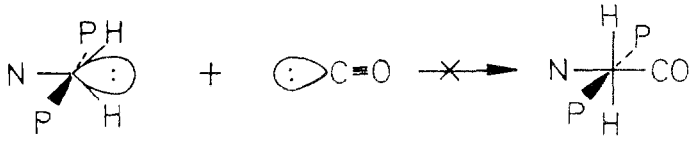

11

bond angle θ. The activation energy for the central attack is about 35 kcal mol^{-1}, a feature of a completely forbidden reaction.

The lateral attack, however, is very favorable. The interaction between CO and the $[Ir]H_2$ complex is gauged by ΔE, a new quantity whose definition is given for the first time in section VII. It is sufficient to note here that the negative and

* Reference numbers with asterisks indicate notes in the list of references.

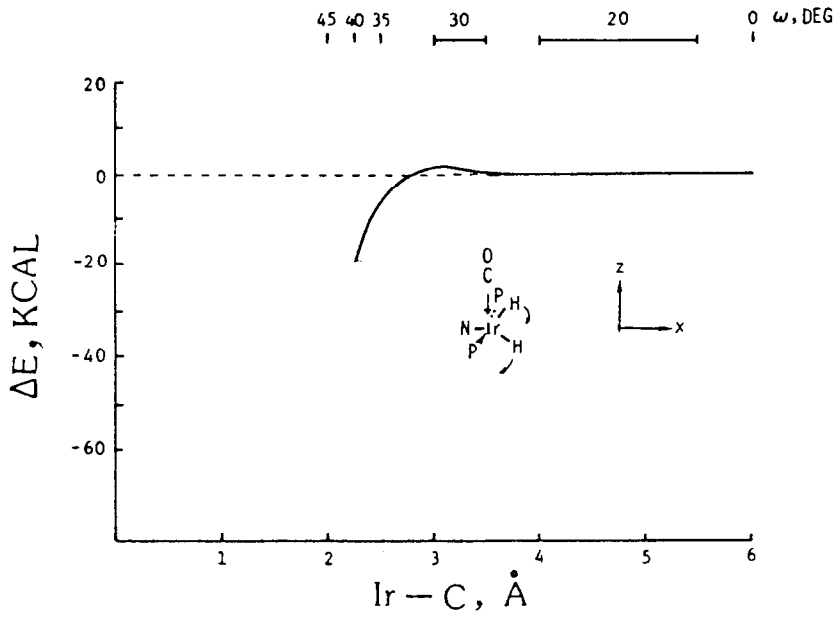

Fig. 3. Energy profile for the lateral attack of CO to $Ir(N(SiH_3)_2)(PH_3)_2H_2$ when the initial structure of the Ir complex is characterized by the local symmetry C_1. The angle ω represents pivoting motion.

positive values of ΔE correspond to stabilizing (attractive) and destabilizing (repulsive) interactions, respectively. Since the Fenske–Hall method (and any single-configuration SCF method or its approximation) is not completely satisfactory for calculation of the energetics of bond formation and dissociation, only initial stages of carbonylation reactions are examined. This procedure proved successful in applications of the extended Hückel method to similar problems [28]. In one mechanism, the $[Ir]H_2$ complex starts with C_{2v} structure. The CO ligand approaches the Ir atom from a direction *trans* to one of the H ligands and the three ligands involved in the reaction, CO and two H atoms, pivot gradually. In the other mechanism, portrayed in Fig. 3, the $[Ir]H_2$ complex starts with the C_1 structure and the pivot angle ω is 20°. The CO ligand approaches along the z axis and the H ligands pivot further. Both of these pathways lead to *mer-cis*-$[Ir]H_2(CO)$ complex, designated **2**. Both of them require minimal activation energies: less than 2 kcal mol^{-1} for the former and about 1 kcal mol^{-1} for the latter. Because of their similarity, the energy profile is shown only for the latter mechanism.

Our findings that the central attack is forbidden and the lateral attack allowed explain why $[Ir]H_2$ reacts easily with CO (and other two-electron donors) to yield **2** as the sole product [19]. The calculations show, however, that stereoselectivity of the reactions does not prove that the structure of $[Ir]H_2$ is rigid. A fluxional complex, too, would react stereoselectively.

IV. Bonding in the zirconium complexes

The electronic structure of bent metallocene complexes Cp_2ML_n has been a subject of various quantum-chemical, structural, and spectroscopic studies [40–57].

The picture of bonding in Cp_2ZrL_2 complexes that emerges from our calculation agrees with the previous findings, so elaboration on this theme would be repetitive. Since we, as well as Lauher and Hoffmann [40], construct a molecule from the Cp_2Zr and L_2 fragments, their incisive study may be consulted for the general features of the electronic structure. (Note that the two studies use different coordinate systems; ours, shown in **12**, is consistent with that shown in **7**. Angles θ and ω also are defined as in **7**.)

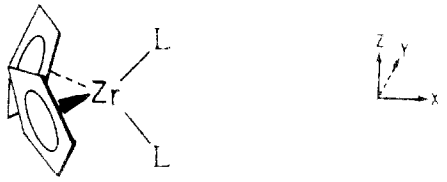

12

Molecular orbital diagrams for Cp_2ZrH_2 and Cp_2ZrCl_2 are given in Figs. 4 and 5, respectively. Since the static electronic structures of the H and Me complexes are similar, Fig. 4 shows the qualitative features of the Me complex as well. In the H and Me compounds the two highest filled orbitals correspond to the Zr–L bonds.

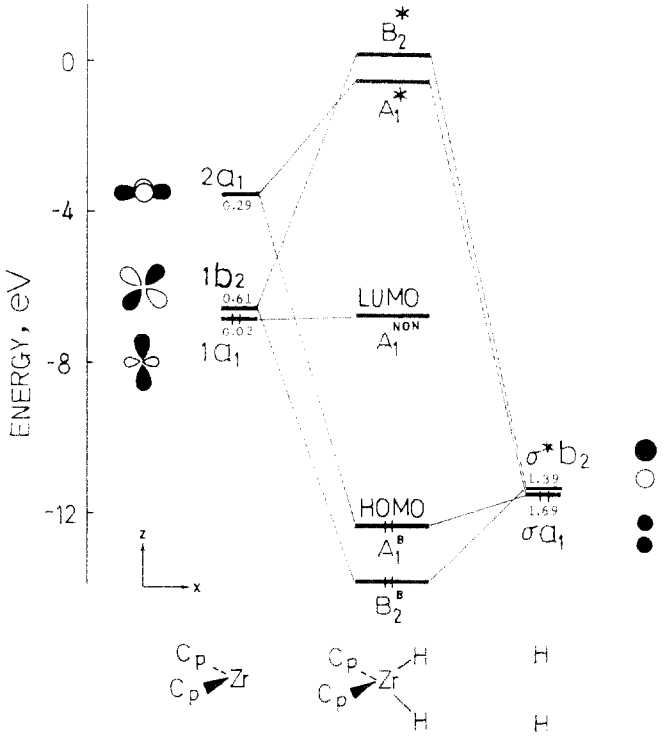

Fig. 4. Molecular-orbital diagram for Cp_2ZrH_2 wherein the HZrH angle is 85°. For explanations, see legend to Fig. 1.

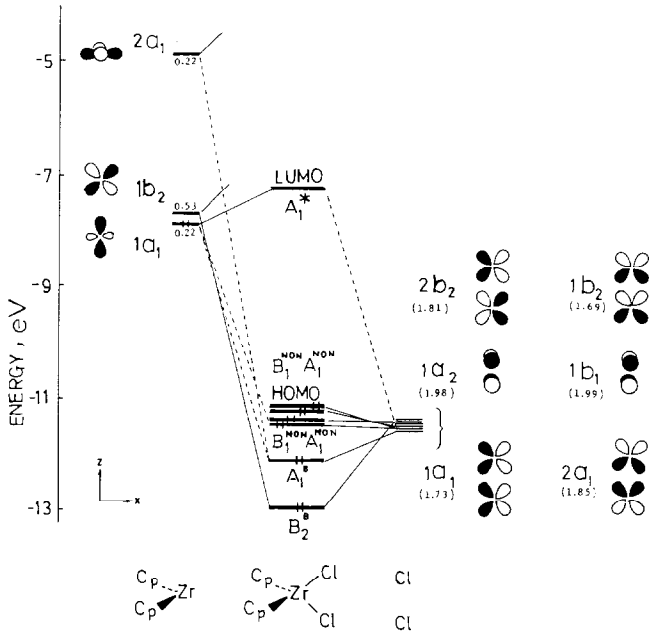

Fig. 5. Molecular-orbital diagram for Cp_2ZrCl_2. The orbitals of the Cl_2 fragment are composed of the atomic p orbitals. For explanations, see legend to Fig. 1.

whereas in the Cl compound there are four lone pairs above the Zr–Cl bonds. The effect of these additional filled orbitals on the reactivity of the Cl complex is discussed in section V.

That the composition of the A_1 orbital, the LUMO in the Zr^{IV} complexes, depends on the LML angle θ has been noted [40,44–47], but the implications of this dependence, shown in Table 3, for the chemical reactivity do not seem to have been fully recognized. As the bond angle opens, a phenomenon likely in view of the steric bulk of the C_5Me_5 ligands, the d_{z^2} character and lateral localization decrease,

Table 3

The compositions of the frontier molecular orbitals in Cp_2ZrH_2 for different values of the HZrH bond angle

Angle, (°)	HOMO		LUMO	
	Zr	H, other	Zr	H
70	8% $d_{x^2-y^2}$	78% 1s	91% d_{z^2} + 2% $d_{x^2-y^2}$	
80	8% $d_{x^2-y^2}$	78% 1s	91% d_{z^2} + 2% $d_{x^2-y^2}$	
90	8% $d_{x^2-y^2}$ + 4% d_{z^2}	84% 1s	78% d_{z^2} + 13% $d_{x^2-y^2}$	
100	5% $d_{x^2-y^2}$ + 9% d_{z^2}	84% 1s	66% d_{z^2} + 22% $d_{x^2-y^2}$	
110	4% $d_{x^2-y^2}$ + 15% d_{z^2}	82% 1s	52% d_{z^2} + 33% $d_{x^2-y^2}$	
120	5% d_{xz}	95% Cp	39% d_{z^2} + 49% $d_{x^2-y^2}$	4% 1s
130	14% d_{xz}	7% 1s + 79% Cp	26% d_{z^2} + 57% $d_{x^2-y^2}$	4% 1s

whereas the $d_{x^2-y^2}$ character and the central localization increase; two limiting cases are shown in **13**.

13

V. Carbonylation of the Cp_2ZrL_2 complexes

VA. Effects of ligands L on reactivity. The three complexes are remarkable for they behave in three different ways toward CO. The Me complex undergoes lateral attack rapidly [25]; the H compound also reacts rapidly, but the attack is central [16,20]; and the Cl complex is unreactive [30]. Our findings on the carbonylation of the Me compound agree with the results of another recent quantum-chemical study of the same reaction [28,29]. Reactions of the other compounds have not been studied so before.

The energy profiles for both the central and lateral approaches of CO to the H, Me, and Cl complexes are given in Fig. 6. Since the outer LML angle in the Cp_2MH_3 complexes of Nb and Ta is 126° [58], and that in the Cp_2ZrH_3 moiety of $[Cp_2ZrH(\mu\text{-}H)]_2$ is 130° [59], the bond angles are varied gradually until the outer angle of 130° is reached in the product, $Cp_2ZrL_2(CO)$. The ΔE criterion again proved useful. The calculated activation energies, ΔE_a, may not be accurate in the absolute sense, but they do permit reliable qualitative comparison of the reactions in which the same ligand, CO, adds to homologous metal complexes, but in different directions.

Our calculations show that Cp_2ZrMe_2 prefers lateral over central attack by about 4 kcal mol^{-1}; the value reported before is 5 kcal mol^{-1} [28]. The central attack on Cp_2ZrH_2 proceeds virtually without a barrier ($\Delta E_a < 2$ kcal mol^{-1}), whereas the lateral attack would have to surmount one of 8 kcal mol^{-1}. The contrast between the H and Me compounds, in concord with experimental facts, cannot be anticipated from the electronic structures of the static compounds themselves, but becomes evident in the treatment of their reactions with the aid of the new ΔE criterion.

A close examination of the orbital interactions between the $[Zr]L_2$ complexes and CO and of the contour plots for the most important interactions reveals a difference between the methyl and hydride complexes in their carbonylation reactions. As would be expected, the crucial interactions are those involving the highest-lying filled and the lowest-lying vacant molecular orbitals of the reactants. In all the cases, the ΔE barrier calculated from this small number of select interactions (especially from the HOMO–LUMO stabilization and the HOMO–HOMO destabilization) was approximately the same as the barrier calculated by inclusion of all the filled molecular orbitals in the reactants. This "localization" of the effects of interest on a relatively small number of orbitals permits a qualitative interpretation

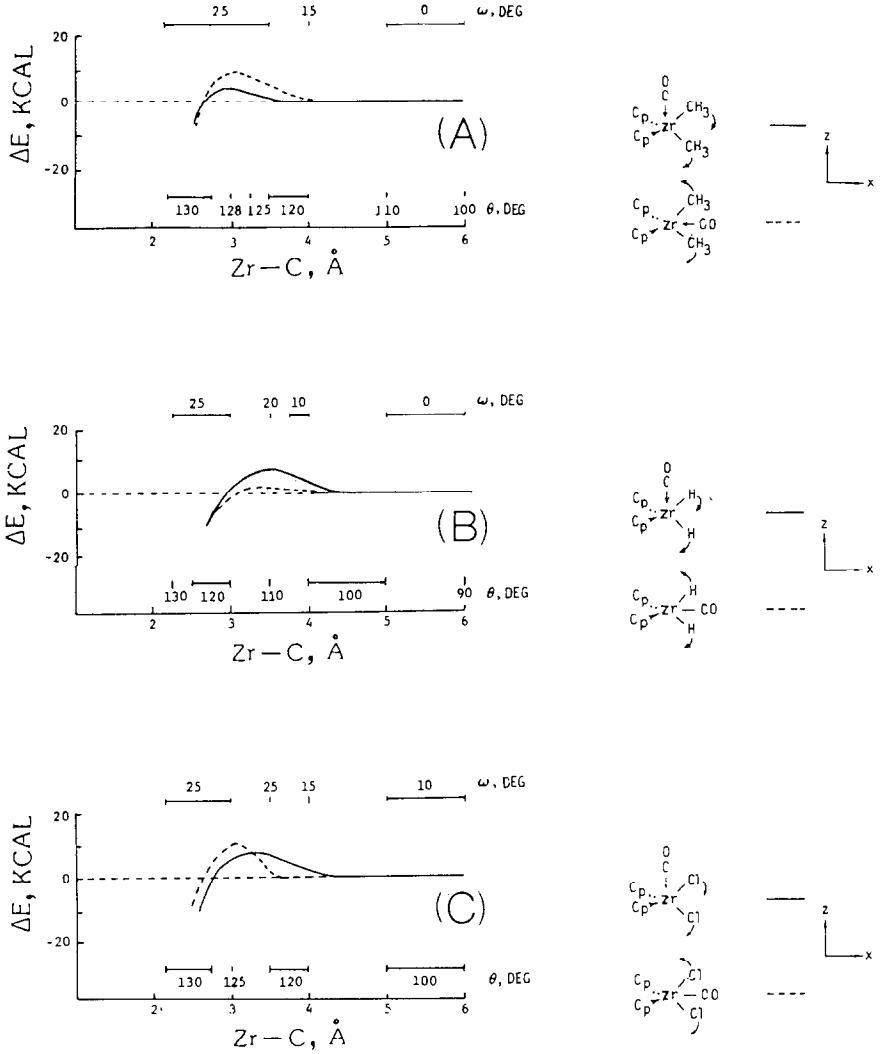

Fig. 6. Energy profiles for the lateral (solid line) and central (dashed line) attacks of CO on: (A) Cp_2ZrMe_2; (B) Cp_2ZrH_2; and (C) Cp_2ZrCl_2. In each case, the ω scale pertains to the lateral and the θ scale, to the central attack.

of the calculated difference between the regioselectivities of the H and Me compounds.

The HOMO, a lone pair, in the entering CO ligand creates a new bond by its interaction with the LUMO of the $[Zr]L_2$ compound, but also feels repulsion from the filled molecular orbitals in this compound. Different repulsive interactions are evident when H and Me are present as ligand L. On the one hand, the Zr–H bond is shorter (1.78 Å) and causes greater accumulation of electron density (the total overlap population between the Zr and H atoms is 0.33 e) than the Zr–Me bond (2.36 Å and 0.28 e, respectively). On the other hand, the filled C–H orbitals in the methyl ligand provide a considerable steric barrier to the CO attack. The central

attack on the H compound seems to be favored by the disposition of the LUMO, i.e., it is frontier-controlled; the lateral attack, in the absence of pivoting, would bring about prohibitive repulsion between the lone pair of CO and the relatively high electron density in the Zr–H bonds. The central attack on the Me compound, although not unfavorable so far as the HOMO–LUMO interaction is concerned, is prohibited by steric repulsions involving the C–H bonds of both Me ligands; the lateral attack is much less hindered by the repulsions involving only one Me ligand.

In the carbonylation of Cp_2ZrCl_2 a barrier cannot be avoided and therefore the complex is unreactive. The calculated ΔE_a values for the central and lateral attacks are 12 and 11 kcal mol^{-1}, respectively. Although these values are not large on the absolute scale and actual barriers of this magnitude might permit a reaction, the ΔE criterion should be used comparatively rather than absolutely, as stated above. These values are even higher than those corresponding to the unfavorable pathways of addition to the Me and H complexes. The barrier seems to originate in the repulsive interactions, shown in **14**, involving the highest filled molecular orbitals in Cp_2ZrCl_2 and the lone pair on the C atom. These interactions, tantamount to steric repulsion, are accentuated by the presence of the bulky Cp rings. The π donation from the π-type lone pairs on the Cl ligands to the Zr atom appears to be rather

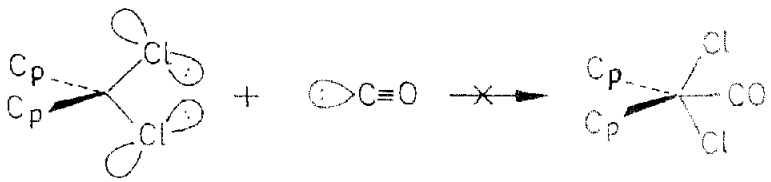

14

weak (the $1a_1$ orbital of the Cp_2Zr fragment is little delocalized on the Cl atoms) and apparently is not the main cause for the unreactivity of Cp_2ZrCl_2 [30].

VB. Bonding in the carbonyl adducts. The new Zr–CO bond in $Cp_2ZrL_2(CO)$ complexes is formed mainly by the relatively weak σ donation from the HOMO of the CO ligand into the LUMO of the Cp_2ZrL_2 complex, orbitals separated by a large energy gap. Hence the easy decarbonylation of $Cp^*_2ZrH_2(CO)$ [16,20] and easy insertion of CO within Cp_2ZrMe_2 [25]. Since the oxidation state of the Zr atom in both Cp_2ZrL_2 and $Cp_2ZrL_2(CO)$ is formally IV and its configuration formally d^0, π back-donation from Zr to CO is not expected. Although the actual (calculated) oxidation state and electron configuration in each of the compounds are close to II and d^2, respectively, the π interaction is indeed absent. The partial occupancy of the d orbitals arises from the partial covalency of the Zr–L bonds and not from the presence of a lone pair that could be back-donated in the conventional sense. The C–O stretching frequency in $Cp_2ZrH_2(CO)$ is nevertheless lower than that in the free CO. Our calculations reveal hyperconjugative interactions between the π^* orbitals of CO and the filled orbitals corresponding to the Zr–H bonds, thus confirming the original hypothesis of Brintzinger and others [30,31]. The primary interaction, shown in **15**, occurs in the xz plane and involves mainly the molecular orbital B_2^B (see Fig. 4) and a π^* orbital of the CO ligand. The secondary interaction, in the xy plane, has B_1 symmetry and involves a molecular orbital of Cp_2ZrH_2 (not shown in Fig. 4) that is localized on the Cp_2Zr fragment and has no

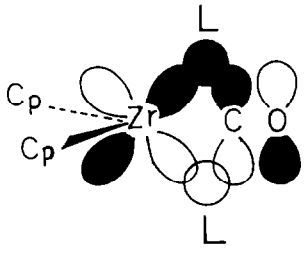

15

contribution from the H ligands. Consequently, the π^* orbitals of CO acquire population of 0.20 e and the C–O stretching frequency is lowered appreciably. Back-donation is also evident, although less pronounced, in $Cp_2ZrMe_2(CO)$, an elusive compound about whose electronic structure there are no experimental data. Since hyperconjugation is manifest in both H and Me complexes, it probably is not an important determinant of their opposite carbonylation reactions.

VI. Theoretical and experimental findings

The ideas developed in this study of carbonylation reactions can also be applied to hydrogenation reactions, although H_2 is not strictly analogous to CO and to other common two-electron donors. In a study of H_2 activation, a lateral attack of H_2 on Cp_2ZrRL complexes was proposed [60,61], but the observed elimination products can be accounted for by virtually the same mechanism involving central attack of H_2 on the Zr atom. The hydrogenation of the complexes containing Cl as L is slower than that of the complexes containing H as L [61], a fact consistent with our view that lone pairs on the ligand retard the addition reaction.

Since the localization of the LUMO in the Cp_2ZrL_2 complexes depend markedly on the LZrL angle, as shown in **13**, the availability of this orbital in the central and lateral directions can, in principle, be controlled experimentally by fixing the bond angle. This can perhaps be achieved in chelates and in metallacycles of different sizes, shown schematically in **16**. A four-membered ring of the former type [62] and four-membered and six-membered rings of the latter type [63] have recently been

SLOW REACTION FAST REACTION

16

reported. The obtuse and acute angle would cause, respectively, central and lateral orientation of the LUMO. Since, in an ideal case, only lateral attack would be allowed sterically, the reactivity should be as indicated in **16**. The chief difficulty in these studies would be to prepare cyclic compounds that cannot undergo central attack and that allow the character of the LUMO to be separated from other influential factors. In particular, these compounds would need to have markedly different bond angles, but similar ligating groups and similar number of lone pairs on the ligands.

In another conceivable study, the effect of lone pairs, which we recognized in the Zr compounds, could be sought in the Ir compounds as well. The halide complex $[Ir]X_2$ should be less reactive than $[Ir]H_2$ with respect to addition of a ligand such as CO. The steric effect of the halide lone pairs, however, should be less pronounced in the Ir complex, which is hexacoordinate, than in the Zr complex, which can be viewed as octacoordinate.

VII. Particulars of the calculations

VIIA. The electronic structure. An approximation to the Hartree–Fock–Roothaan technique, the Fenske–Hall method, has been described elsewhere [64]. This iterative SCF method is devoid of empirical or adjustable parameters, so that results of a calculation (eigenvalues, eigenvectors, and the derived quantities) are determined fully by the molecular geometry and basis functions. In the computation of the Fock matrix elements, the small but significant effects of the intramolecular electrostatic interactions are taken into account. Consequently, the energies of the fragment orbitals reflect the influences of the molecular environment on the fragments "ready for bonding". This realistic aspect of our calculations is exemplified in Fig. 4 and 5, which show that the Cp_2Zr fragment has slightly different bonding properties, mainly the orbital energies, when it interacts with H and with Cl ligands. These features of the method add to its usefulness for the construction of reaction profiles and for the study of large molecules of low symmetry.

The structure of the Ir-containing fragment [37]; the Ir–H bond distances [36]; the structure of the Cp_2Zr fragment [65]; and the Zr–H [59], Zr–Me [66], Zr–Cl [67], and Zr–CO [68] bond distances were taken from the actual compounds. The usual basis functions were used for the metal [69], nonmetal [70], and H [71] atoms. Occupations of the fragment orbitals and atomic charges were calculated by the Mulliken population analysis.

In view of the size and complexity of the molecules studied, only partial optimization of their geometric structures was feasible. Those bond angles and distances that are immediately affected by the carbonylation reactions were allowed to relax. The angles ω and θ in the starting $[M]L_2$ complexes were optimized by minimization of the summed energy of the filled molecular orbitals [72]. The angle θ or ω and the M–CO distance in the reactions were varied as shown in Fig. 3 and 6. The ΔE criterion was used only for following the reactions, not for optimization of the geometric structures.

VIIB. Definition and meaning of ΔE. In order to elucidate bonding in the complex molecules and to compare various modes of the carbonylation reactions, we carried out transformations of the basis sets. After an iterative calculation on a large fragment, a molecule, or a reaction system would converge with the basis set of

atoms or of smaller fragments, the molecular orbitals would be transformed into the basis set of larger fragments or of reactants (the metal complex and CO). Without affecting the numerical results of the calculations, these transformations facilitate their interpretation.

The quantity ΔE is defined for the first time below. Let a system consist of fragments A and B, so that the orbitals of the system are expressed in terms of fragment orbitals, ϕ_i and ϕ_j. Atoms in A and B are designated a and b, respectively. Then,

$$\langle \phi_i \mid \phi_j \rangle = \begin{cases} \delta_{ij} \text{ if } \phi_i, \phi_j \in \mathrm{A} \\ S_{ij} \text{ if } \phi_i \in \mathrm{A}, \phi_j \in \mathrm{B} \end{cases} \tag{4}$$

Fock matrix in the block form

$$\begin{bmatrix} F_{ii}^{\mathrm{AA}} & F_{ij}^{\mathrm{AB}} \\ F_{ji}^{\mathrm{BA}} & F_{jj}^{\mathrm{BB}} \end{bmatrix}$$

The original expressions [64] for the matrix elements in the transformed basis become:

$$F_{ii}^{\mathrm{AA}} = \lambda_i^{\mathrm{A}} + \sum_b \left(-\frac{Q_b}{R_{ab}} \right) \tag{5}$$

$$F_{ij}^{\mathrm{AA}} = 0 \tag{6}$$

$$F_{ij}^{\mathrm{AB}} = S_{ij}\left(\lambda_i^{\mathrm{A}} + \lambda_j^{\mathrm{B}}\right) - \langle \phi_i^{\mathrm{A}} \mid -\tfrac{1}{2}\nabla^2 \mid \phi_j^{\mathrm{B}} \rangle \tag{7}$$

where λ_i represents the ith eigenvalue of fragment A and the second term in eq. 5 represents Madelung interactions involving an electron in ϕ_i^{A} and all the other atoms b in fragment B. Define ΔE for a case of two fragments:

$$\Delta E = \sum_{k=1}^{\mathrm{occ}} \lambda_k - \left[\sum_{i=1}^{\mathrm{occ}} F_{ii}^{\mathrm{AA}} + \sum_{j=1}^{\mathrm{occ}} F_{jj}^{\mathrm{BB}} \right] \tag{8}$$

(An analogous expression can be written for a case of many fragments; the second term then becomes a double summation, $\sum_{\mathrm{A}} \sum_{i=1}^{\mathrm{occ}} F_{ii}^{\mathrm{AA}}$.) From eq. 5,

$$\Delta E = \sum_{k=1}^{\mathrm{occ}} \lambda_k - \left[\sum_{i=1}^{\mathrm{occ}} \lambda_i^{\mathrm{A}} + \sum_{j=1}^{\mathrm{occ}} \lambda_j^{\mathrm{B}} + N_a \sum_b \left(\frac{Q_b}{R_{ab}} \right) + N_b \sum_a \left(\frac{Q_a}{R_{ab}} \right) \right] \tag{9}$$

where N_a and N_b represent the numbers of valence electrons in the fragments A and B, respectively.

The difference between the orbital energies of the proximate and separate reactants A and B, which ΔE evidently is, reflects the electronic interactions, both attractive and repulsive, between the reactants. The orbital energies, λ_k, of the "supermolecule" A...B include, of course, the off-diagonal matrix elements, defined in eq. 7. If the distance R_{ab} is long, A and B do not interact and conditions in

$$F_{ii}^{\mathrm{AA}} = \lambda_i^{\mathrm{A}} \qquad F_{ij}^{\mathrm{AB}} = 0 \qquad \Delta E = 0 \tag{10}$$

eq. 10 obtain. If the molecules interact, $F_{ij}^{\mathrm{AB}} \neq 0$ and $\Delta E \neq 0$. In particular, $\Delta E > 0$

and $\Delta E < 0$ correspond, respectively, to net repulsion and net attraction between the fragments.

Since the Fenske–Hall method does not include internuclear repulsions (a limitation common to most of the nonrigorous molecular orbital methods), the ΔE does not necessarily reach a minimum as the AB distance decreases. This is why the ΔE criterion should be used only for the initial stages of a reaction. The new criterion is nevertheless more reliable than the one based on simple minimization of the summed orbital energies, $\Sigma\lambda_k$. Whereas the quantity ΔE reflects the relative (de)stabilization of A...B in comparison with A + B, the sum $\Sigma\lambda_k$ would be an ill-justified approximation to an absolute total energy of the reactants. One of the advantages of the Fenske–Hall method is that λ_j^A and λ_j^B are not "frozen": the interactions in A...B alter them. This realistic aspect of the present calculations enhances their usefulness in the ΔE method, but would detract from their reliability if the $\Sigma\lambda_k$ method were to be used.

Acknowledgments

We thank Professors J.E. Bercaw of Caltech, J.L. Petersen of West Virginia University, J. Schwartz of Princeton University, and M.D. Fryzuk of the University of British Columbia, who commented on this work. The research was supported by Iowa State University and its Computation Center. One of us, L.Z., thanks Nanjing University, People's Republic of China, for a leave of absence.

References and Notes

1 B.R. James, Homogeneous Hydrogenation, Wiley, New York, 1973.
2 See the papers presented at the Symposium on Hydrogen-Rich Organometallic and Inorganic Complexes, 191st National Meeting of the American Chemical Society, New York City, 13–18 April, 1986.
3 J.P. Brothers, Prog. Inorg. Chem., 28 (1981) 1.
4 G.J. Kubas, J. Chem. Soc., Chem. Commun., (1980) 61.
5 G.J. Kubas, R.R. Ryan, B.I. Swanson, P.J. Vergamini and H.J. Wasserman, J. Am. Chem. Soc., 106 (1984), 451.
6 (a) G.J. Kubas, R.R. Ryan and D.A. Wrobleski, J. Am. Chem. Soc., 108 (1986) 1339; (b) H.C. Clark and M.J.J. Hampden-Smith, ibid., 108 (1986) 3829.
7 H.J. Wasserman, G.J. Kubas and R.R. Ryan, J. Am. Chem. Soc., 108 (1986) 2294.
8 (a) R.K. Upmacis, G.E. Gadd, M. Poliakoff, M.B. Simpson, J.J. Turner, R. Whyman and A.F. Simpson, J. Chem. Soc., Chem. Commun., 106 (1985) 27; (b) R.K. Upmacis, M. Poliakoff and J.J. Turner, J. Am. Chem. Soc., 108 (1986) 3645.
9 G.E. Gadd, R.K. Upmacis, M. Poliakoff and J.J. Turner, J. Am. Chem. Soc., 108 (1986) 2547.
10 R.H. Crabtree and M. Lavin, J. Chem. Soc., Chem. Commun., (1985) 794.
11 R.L. Sweany, J. Am. Chem. Soc., 107 (1985) 2374.
12 R.L. Sweany, Organometallics, 5 (1986) 387.
13 S.P. Church, F.-W. Grevels, H. Herrmann and K. Schaffner, J. Chem. Soc., Chem. Commun., (1985), 30.
14 R.H. Morris, J.F. Sawyer, M. Shiralian and J.D. Zubkowski, J. Am. Chem. Soc., 107 (1985) 5581.
15 F.M. Conroy-Lewis and S.J. Simpson, J. Chem. Soc., Chem. Commun., (1986) 506.
16 P.T. Wolczanski and J.E. Bercaw, Acc. Chem. Res., 13 (1980) 121 and ref. cited therein.
17 K.S. Wong, W.R. Scheidt and J.A. Labinger, J. Am. Chem. Soc., 100 (1978) 3254.
18 D.B. Carr and J. Schwartz, J. Am. Chem. Soc., 101 (1979) 3521.
19 M.D. Fryzuk and P.A. MacNeil, Organometallics, 2 (1983) 682.
20 J.M. Manriquez, D.R. McAlister, R.D. Sanner and J.E. Bercaw, J. Am. Chem. Soc., 100 (1978) 2716.
21 M.D. Fryzuk, private communication to N.M.K.
22 P.T. Wolczanski, R.S. Threlkel and J.E. Bercaw, J. Am. Chem. Soc., 101 (1979) 218.

23 P.T. Wolczanski and J.E. Bercaw, J. Am. Chem. Soc., 101 (1979) 6450.
24 G. Erker, U. Dorf, P. Czisch and J.L. Petersen, Organometallics, 5 (1986) 668.
25 G. Erker, Acc. Chem. Res., 17 (1984) 103 and ref. cited therein.
26 G. Erker and F. Rosenfeldt, J. Organomet. Chem., 188 (1980) C1.
27 G. Erker and F. Rosenfeldt, Angew. Chem., Int. Ed. Engl., 17 (1978) 605.
28 K. Tatsumi, A. Nakamura, P. Hofmann, P. Stauffert and R. Hoffmann, J. Am. Chem. Soc., 107 (1985) 4440.
29 P. Hofmann, P. Stauffert, K. Tatsumi, A. Nakamura and R. Hoffmann, Organometallics, 4 (1985) 404.
30 J.A. Marsella, C.J. Curtis, J.E. Bercaw and K.G. Caulton, J. Am. Chem. Soc., 102 (1980) 7244.
31 H.H. Brintzinger, J. Organomet. Chem., 171 (1979) 337.
32 P.J. Hay, Chem. Phys. Lett., 103 (1984) 466.
33 J.-Y. Saillard and R. Hoffmann, J. Am. Chem. Soc., 106 (1984) 2006.
34 A.R. Rossi and R. Hoffmann, Inorg. Chem., 14 (1975) 365.
35 J.K. Burdett, Molecular Shapes, Wiley-Interscience, New York, 1980, p. 189–190.
36 M.D. Fryzuk, P.A. MacNeil and S.J. Rettig, Organometallics, 4 (1985) 1145 and ref. 8 cited therein.
37 M.D. Fryzuk, P.A. MacNeil and S.J. Rettig, J. Am. Chem. Soc., 107 (1985) 6708.
38 M.D. Fryzuk, P.A. MacNeil and R.G. Ball, J. Am. Chem. Soc., 108 (1986) 6414.
39 The structure probably is not very close to a square pyramid; such a large distortion would be manifest in the nuclear Overhauser effect.
40 J.W. Lauher and R. Hoffmann, J. Am. Chem. Soc., 98 (1976) 1729.
41 A. Veillard, Nouv. J. Chim., 5 (1981) 599.
42 H.H. Brintzinger, L.L. Lohr, Jr. and K.L.T. Wong, J. Am. Chem. Soc., 97 (1975) 5146.
43 H.H. Brintzinger and L.S. Bartell, J. Am. Chem. Soc., 92 (1970) 1105.
44 J.L. Petersen and L.F. Dahl, J. Am. Chem. Soc., 97 (1975) 6416.
45 J.L. Petersen and L.F. Dahl, J. Am. Chem. Soc., 97 (1975) 6422.
46 J.L. Petersen, D.L., Lichtenberger, R.F. Fenske and L.F. Dahl, J. Am. Chem. Soc., 97 (1975) 6433.
47 J.L. Petersen and L.F. Dahl, J. Am. Chem. Soc., 96 (1974) 2248.
48 C.P. Stewart and A.L. Porte, J. Chem. Soc., Dalton Trans., (1973) 722.
49 D.P. Bakalik and R.G. Hayes, Inorg. Chem., 11 (1972) 1734.
50 N.W. Alcock, J. Chem. Soc. A, (1967), 2001.
51 J.C.W. Chien, J. Phys. Chem., 67 (1963) 2477.
52 C.J. Ballhausen and J.P. Dahl, Acta Chem. Scand., 15 (1961) 1333.
53 H. Van Dam, A. Terpstra, A. Oskam and J.H. Teuben, Z. Naturforsch. B, 36 (1981) 420.
54 C. Cauletti, J.P. Clark, J.C. Green, S.E. Jackson, I.L. Fragala, E. Gilberto and A.W. Coleman, J. Electron Spectr., 18 (1980) 61.
55 J.C. Green, S.E. Jackson and B. Higginson, J. Chem. Soc., Dalton Trans., (1975) 403.
56 M.L.H. Green, Pure Appl. Chem., 30 (1972) 373.
57 J.C. Green, M.L.H. Green and C.K. Prout, J. Chem. Soc., Chem. Commun., (1972) 421.
58 R.D. Wilson, T.F. Koetzle, D.W. Hart, A. Kvick, D.L. Tipton and R. Bau, J. Am. Chem. Soc., 99 (1977) 1775.
59 S.B. Jones and J.L. Petersen, Inorg. Chem., 20 (1981) 2889.
60 K.I. Gell and J. Schwartz, J. Am. Chem. Soc., 100, (1978), 3246.
61 K.I. Gell, B. Posin, J. Schwartz and G.M. Williams, J. Am. Chem. Soc., 104 (1982) 1846.
62 R.T. Baker and T.H. Tulip, Organometallics, 5 (1986) 839.
63 G. Erker, T. Mühlenbernd, R. Benn, A. Rufińska, G. Tainturier and B. Gautheron, Organometallics, 5 (1986) 1023.
64 M.B. Hall and R.F. Fenske, Inorg. Chem., 11 (1972) 768.
65 J.L. Atwood, R.D. Rogers, W.E. Hunter, C. Floriani, G. Fachinetti and A. Chiesi-Villa, Inorg. Chem., 19 (1980) 3813.
66 W.E. Hunter, D.C. Hrncir, R.V. Bynum, R.A. Penttila and J.L. Atwood, Organometallics, 2 (1983) 750.
67 N.J. Wells, J.C. Huffman and K.G. Caulton, J. Organomet. Chem., 213 (1981) C17.
68 D.J. Sikora, M.D. Rausch, R.D. Rogers, J.L. Atwood, J. Am. Chem. Soc., 103 (1981) 1265.
69 H. Basch and H.B. Gray, Theoret. Chim. Acta (Berlin), 4 (1966) 367.
70 E. Clementi, J. Chem. Phys., 40 (1964) 1944.
71 W.J. Hehre, R.F. Stewart and J.A. Pople, J. Chem. Phys., 51 (1969) 2657.
72 N.M. Kostić and R.F. Fenske, J. Am. Chem. Soc., 104 (1982) 3879 and ref. 15 cited therein.